[1]Mihir Chaudhari
[2]Nirav D. Patel
[3]Priyank R. Bhavsar
[4]Ashok L. Vaghamshi
[5]Dr I. N. Trivedi

Study of Partial Shading Effect on the Different Photovoltaic Array Arrangements and their Shade Resilience

Journal of Electrical Systems

Abstract: - Due to its ability to directly and cleanly convert solar radiation into electricity, the use of photovoltaic (PV) technology is rapidly increasing. Solar PV panels are connected in various series and parallel configurations to achieve the necessary output voltages and currents. They perform optimally when completely unshaded, but when a series connection is partially shaded (PS), bypass diodes activate and the overall voltage drops, resulting in reduced power generation. The location of bypass diodes, series-parallel combination types, and shading patterns all impact the output power. Therefore, selecting the appropriate PV panel arrangement can potentially increase output under these conditions. This study analyzes the shade resilience ability of series-parallel (SP), Total cross-tied (TCT), Bridge-linked (BL), and Honeycomb (HC) configurations.

Keywords: Partially shaded Condition, Photovoltaic Array, Power Loss, PV configurations

I. INTRODUCTION

Various factors such as tree leaves, bird droppings, clouds, and the shade of a building or tree can cause partial shading, impacting the performance of solar panels or cells connected in series. When cells in a series are partially shaded, they may experience reverse biasing and drain their power while operating as a load, potentially leading to hot spots if the system lacks protection. To address this issue, bypass diodes can be used to maintain a constant string current by bypassing shaded cells. This results in the solar array's P-V characteristics displaying several peaks, which may require Maximum Power Point (MPP) Algorithms to identify local peaks rather than global ones. Different methodologies are used to track the global Maximum PowerPoint (GMPP) under partially shaded conditions.

The yearly electricity production in PV parks is reduced by 3-6% due to partial shading losses [1]. This study utilizes MATLAB/Simulink to simulate partial shading in SP, TCT, BL, and HC setups. The study investigates the performance of different configurations about shading losses and GMPP. It includes simulations for every scenario involving partial shading.

The document is organized as follows: Section II covers the mathematical model of the photovoltaic cells. Section III presents the theory of analysis utilized in this paper. Section IV displays the various shading patterns used for the study. Section V reviews the results, and Section VI covers the conclusion.

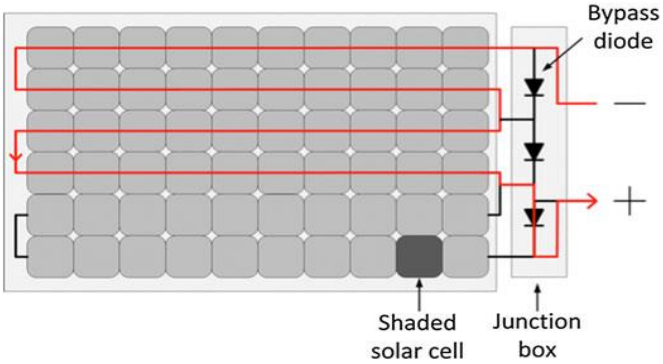

Fig. 1. Panel with 60 cells in series [2]

[1]Electrical Engineering Department, GEC, Gandhinagar, mihirchaudhari@gecg28.ac.in
[2]Electrical Engineering Department, GEC, Gandhinagar, niravdpatel@gecg28.ac.in
[3]Electrical Engineering Department, GEC, Gandhinagar, prbhavsar@gecg28.ac.in
[4]Electrical Engineering Department, GEC, Gandhinagar, ashokvaghamshi@gecg28.ac.in
[5]Vishwakarma Government Engineering College, Power Electronics Department, Chandkheda,int@vgec.ac.in

II. MATHEMATICAL MODEL

The literature has a variety of electrical equivalents for photovoltaic cells and panels. However, the one-diode model seen in Fig. 2 is the most popular.

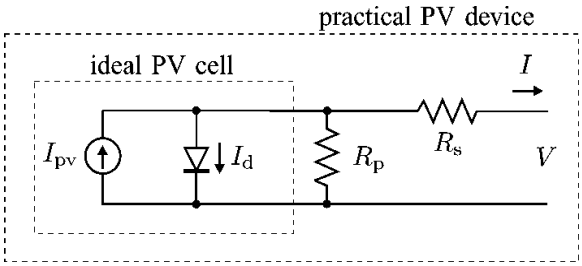

Fig 2. Practical PV Panel [3]

The basic semiconductor theory equation [3] that provides the I–V characteristic of the perfect PV cell mathematically is

$$I= I_{pv,\,cell} - I_{0,\,cell}\left[\exp\left(\frac{qV}{akT}\right)-1\right] \quad (1)$$

where $\left[\exp\left(\frac{qV}{akT}\right)-1\right]=I_{d,}$ $I_{pv,\,cell}$ is the current generated by the incident light (it is directly proportional to the Sun irradiation), I_d is the Shockley diode equation, $I_{0,\,cell}$ is the reverse saturation or leakage current of the diode, q is the electron charge ($1.60217646 \times 10^{-19}$ C), k is the Boltzmann constant ($1.3806503 \times 10^{-23}$ J/K), T (in Kelvin) is the temperature of the *p–n* junction, a is the diode ideality constant.

The PV cell's equation (1) and the realistic PV array's I–V characteristics differ. Since PV arrays have series-connected PV cells, the fundamental equation must be modified to account for extra parameters to obtain the attributes at the PV array's terminals. [3]

$$I= I_{pv} - I_0\left[\exp\left(\frac{V+RsI}{Vta}\right)-1\right]-\frac{V+IRs}{Rp} \quad (2)$$

where I_{pv} and I_0 are the photovoltaic (PV) and saturation currents, respectively, and $V_t = N_skT/q$ is the thermal voltage of the array. N_s is the number of cells connected in a series.

Series connected cells produce higher output voltages, and parallel connected cells boost current in the PV array. The PV and saturation currents for various N_p parallel linked cells are expressed as $I_{pv} = I_{pv,cell}N_p$ and $I_0 = I_{0,cell}N_p$.

R_p is the array's equivalent parallel resistance, and R_s is its analogous series resistance.

The Matlab-Simulink model of the Topsun 240W panel was created using this one-diode model.

All the parameters listed in the Topsun datasheet displayed in Table I are used to validate this mathematical model. The outcome of the simulation at STC matches the datasheet exactly. When I-V and P-V curves of the Matlab model and datasheet and are examined, they match perfectly.

Table 1. Topsun 240W panel data sheet (STC)

MODEL	P_{max} (W)	V_{mp} (V)	I_{mp} (A)	V_{oc} (V)	I_{sc} (A)	Eff %
240W	240	30	8.09	36	8.78	14.84

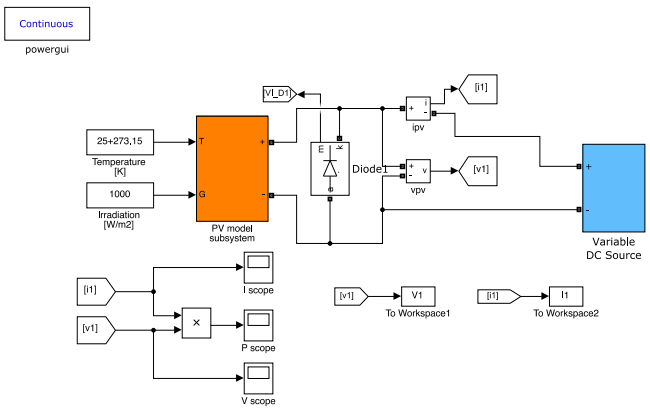

Fig 3. Matlab / Simulink model of Topsun 240W PV Panel

III. THEORY OF ANALYSIS

The simulations were conducted for all four setup types using a variety of potential shade patterns. A 4x4 panel configuration was utilised for the simulations, with each setup using the same shade pattern. Each shade pattern was then compared with its corresponding GMPP. The arrangement that produced the highest GMPP outperformed the others for a given shade pattern. The connection diagram for the SP, TCT, BL, and HC arrangement is depicted in the figure.

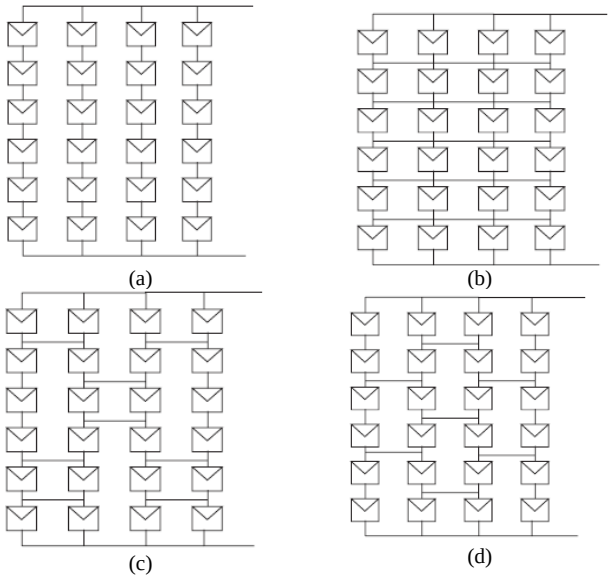

Fig. 4. Schematic diagram of (a) SP, (b) TCT, (c) HC, and (d) BL [3]

The modules are connected in series, and then these parallel series strings are joined with ties between the bridges in TCT. Voltage and current values are obtained by connecting panels in series and currents in parallel [5].

Scientists rarely use the honeycomb layout. The Bridge Link is a modified Honey Comb (HC) construction that combines the advantages of TCT and BL configurations in the HC configuration [5].

IV. PATTERNS OF SHADE

The simulation presents various shade patterns in the figure below, with a 4x4 square representing the 16 solar panels. Shaded panels have an irradiation of 100 W/m^2, while non-shaded panels have an irradiation of 800 W/m2. Patterns 1 through 5 show partially shaded columns, and patterns 6 through 9 depict row-wise partial shading conditions. In Pattern 10, diagonally placed panels are shaded. Patterns 11 through 16 involve shifting clouds, with a top right corner indicating the arrival of the cloud and a bottom left corner indicating its departure. The cloud's centre has an irradiation of 80 W/m^2, while the outside is exposed to 400 W/m^2.

For Patterns 17 through 20, different scattered cloud conditions are considered, with an irradiation of 400 W/m^2 outside and 80 W/m^2 in the centre. Patterns 17 and 18 are similar, but in Pattern 18, the cloud's centre is located in the panel's corner. Pattern 19 shows all 16 panels having the same shade, while Pattern 20 displays scattering clouds with varying irradiations of 600 W/m^2, 450 W/m^2, and 150 W/m^2.

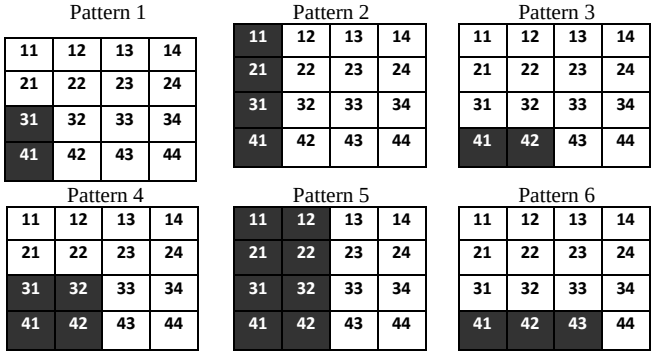

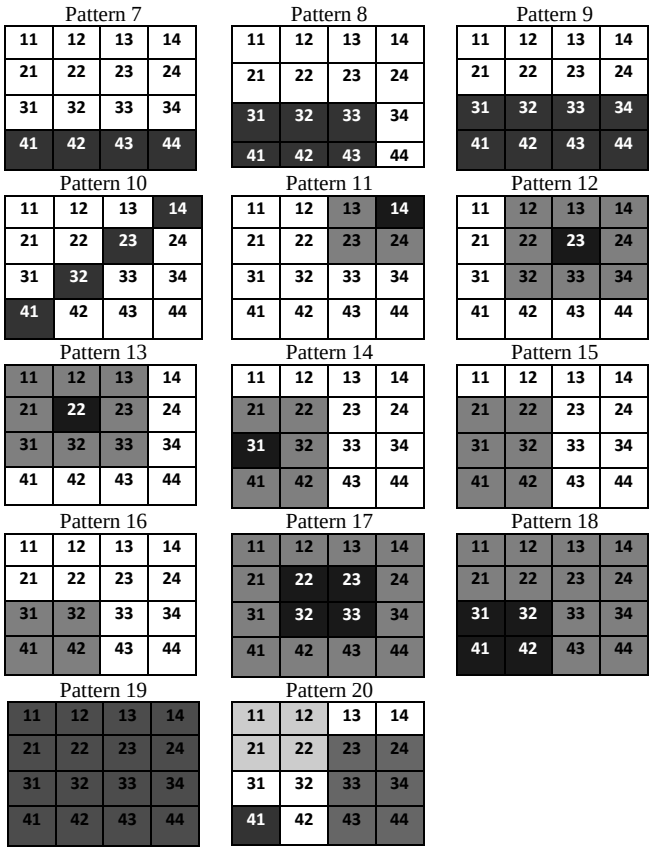

Fig 5. Different Shading Patterns are used

V. OUTCOME AND TALK

Under typical operating conditions, a temperature reading of 45°C and an 800 W/m^2 irradiation were recorded. The temperature remains at 45°C for Patterns 1 through 20.

The findings are presented in Table 2.

Irradiation level is grapphically represented for each shading pattern in this table. Each shading pattern is simulated for SP, TCT, BL and HC combinations. GMPPT is recorded for the each pattern and it is grapgically presented in this table.

Table 2. Outputs according to shade pattern

Pattern No.	Irradiation level on 4x4 Panels	Output of different configurations
1	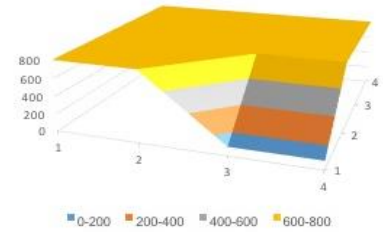	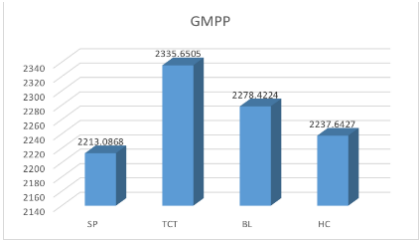
2	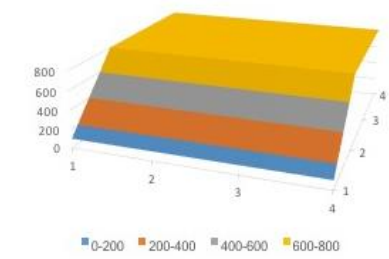	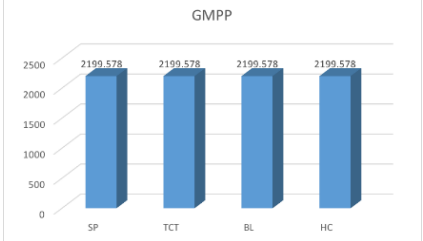

3

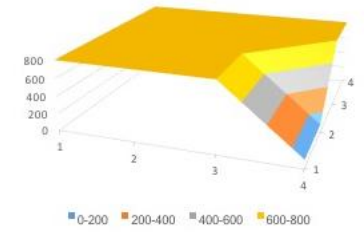
800
600
400
200
0
0-200
200-400
400-600
600-800

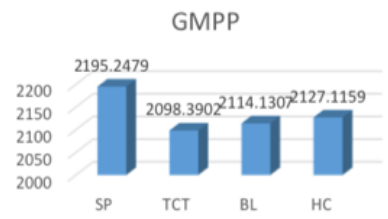
GMPP
2195.2479
2098.3902
2114.1307
2127.1159
2200
2150
2100
2050
2000
SP
TCT
BL
HC

4

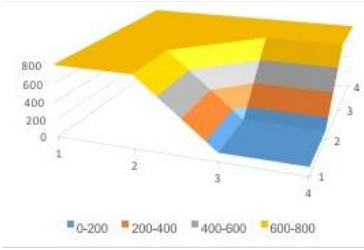
800
600
400
200
0
0-200
200-400
400-600
600-800

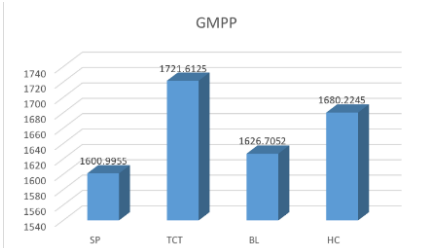
GMPP
1600.9955
1721.6125
1626.7052
1680.2245
SP
TCT
BL
HC

5

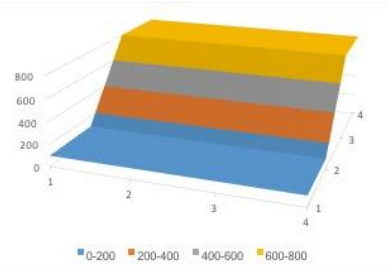
800
600
400
200
0
0-200
200-400
400-600
600-800

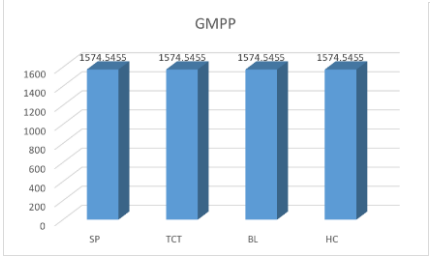
GMPP
1574.5455
1574.5455
1574.5455
1574.5455
SP
TCT
BL
HC

6

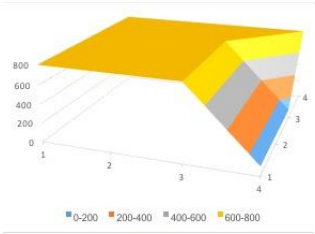
800
600
400
200
0
0-200
200-400
400-600
600-800

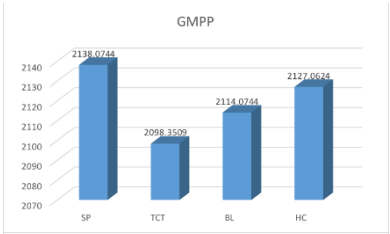
GMPP
2138.0744
2098.3509
2114.0744
2127.0624
SP
TCT
BL
HC

7

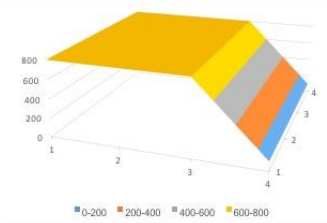
800
600
400
200
0
0-200
200-400
400-600
600-800

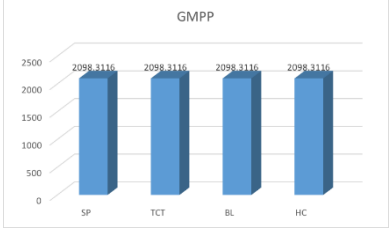
GMPP
2098.3116
2098.3116
2098.3116
2098.3116
SP
TCT
BL
HC

8

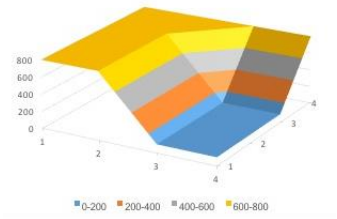
800
600
400
200
0
0-200
200-400
400-600
600-800

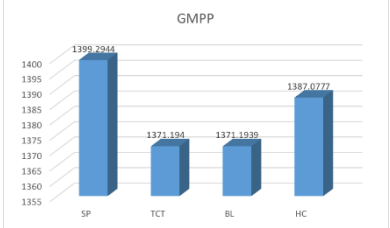
GMPP
1399.2944
1371.194
1371.1939
1387.0777
SP
TCT
BL
HC

9

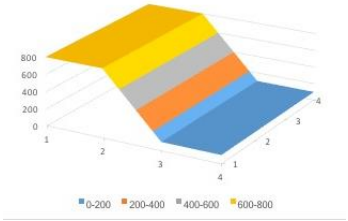
800
600
400
200
0
0-200
200-400
400-600
600-800

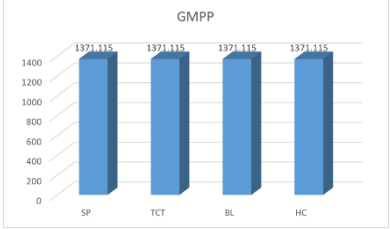
GMPP
1371.115
1371.115
1371.115
1371.115
SP
TCT
BL
HC

10

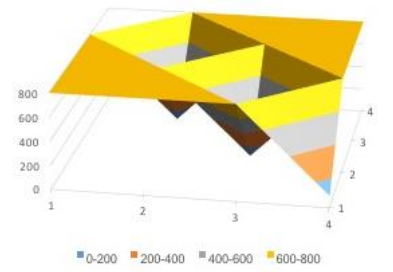

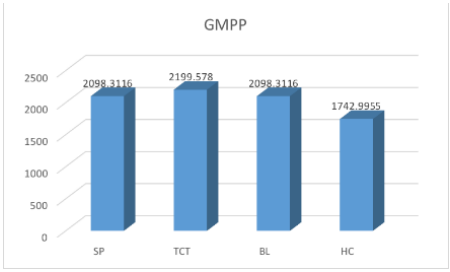

11

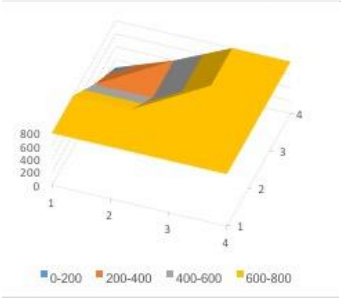

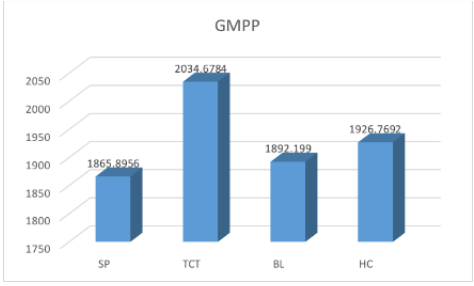

12

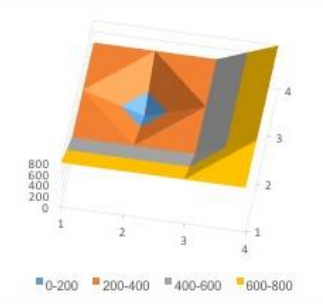

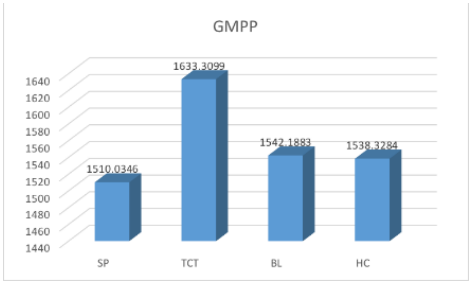

13

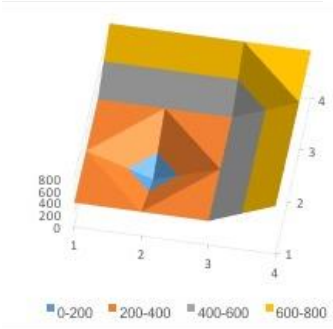

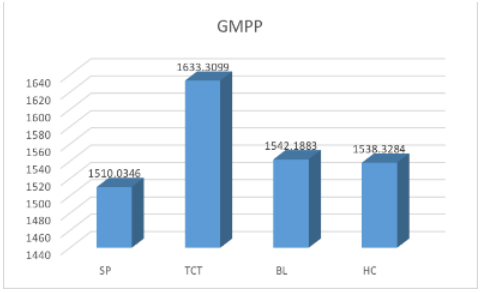

14

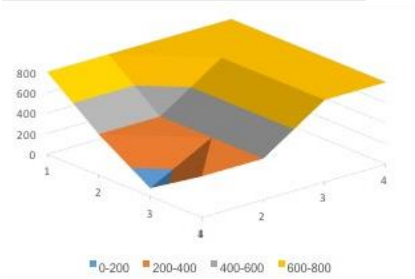

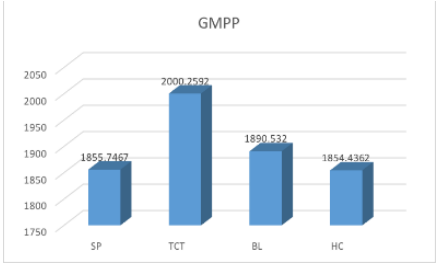

15

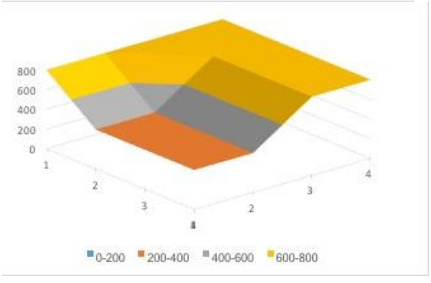

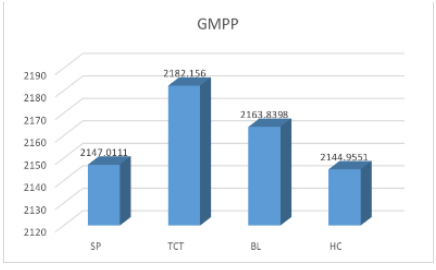

16

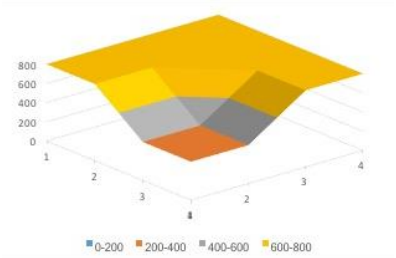

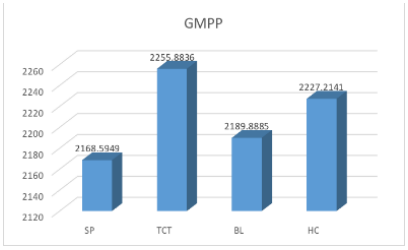

17

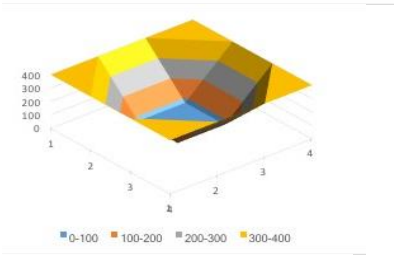

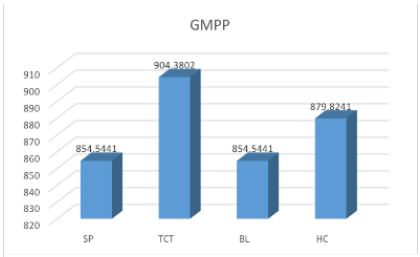

18

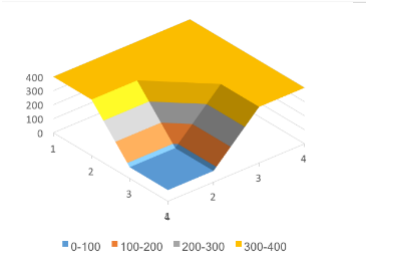

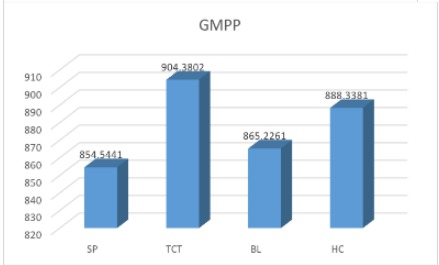

19

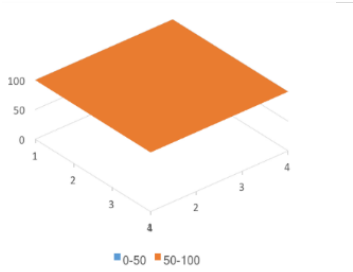

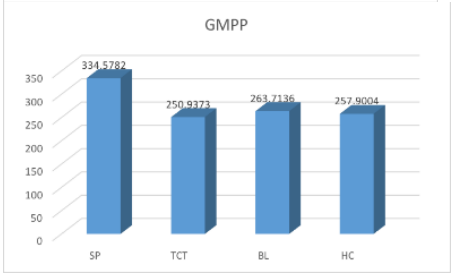

20

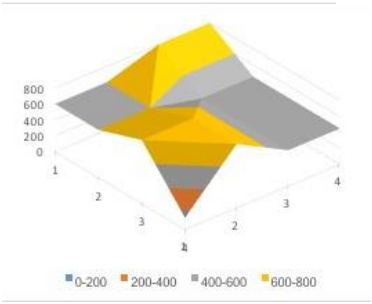

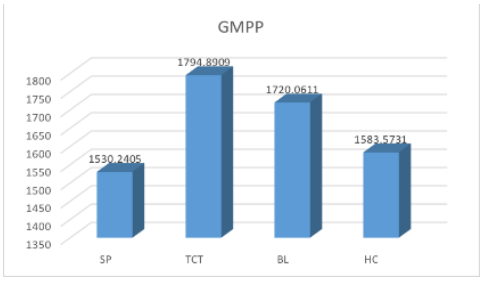

A. Row, Column and Diagonal Shading

In Pattern 1, TCT has the highest GMPP, SP has the lowest GMPP, and BL and HC are in the second and third positions.

Pattern 2's GMPP of all 4-panel configurations is the same due to the uniform shading.

In Pattern 3, SP has the highest GMPP, and TCT has the lowest GMPP due to row-wise shading. HC and BL are in second and third positions, respectively.

For Pattern 5, because of uniform shading conditions, the GMPP of all the 4-panel configurations are the same.

In Pattern 6, the GMPP of SP is highest, and TCT is lowest due to row-wise shading. HC and BL are in second and third positions.

Pattern 7's GMPP of all configurations is the same due to the balanced shading condition.

In Pattern 8, the GMPP of SP is highest. TCT and BL have the lowest GMPP due to the shade in the row. HC is in the second position.

Pattern 9's GMPP of all configurations is the same due to uniform shading conditions.

In Pattern 10, the GMPP of the TCT configuration is high, and the HC configuration is low. SP and BL configurations have the same GMPP.

B. Moving Cloud Condition

The TCT configuration has the highest GMPP in Pattern 11, while the SP configuration has the lowest. In Patterns 12 and 13, TCT has the highest GMPP, and SP has the lowest. In cases 14 and 15, TCT has the highest GMPP, and HC has the lowest GMPP. In case 16, TCT has the highest GMPP and SP has the lowest.

C. Cloud covering all the panels

Pattern 17 has the highest GMPP among the TCT, while SP has the lowest GMPP.

D. Selecting a Template (Heading 2)The center of the cloud at the corner of the panel.

Pattern 18's TCT has the highest GMPP, while SP has the lowest.

E. All the panels are uniformly shaded

Pattern 19 consists of 16 uniformly shaded panels. SP has the highest, and TCT has the lowest GMPP, with a slightly marginal difference.

F. Scattered clouds

In Pattern 20, TCT has the highest GMPP, and SP has the lowest GMPP

VI. CONCLUSION

In Patterns 1, 4, 11 to 18, and 20, the TCT configuration consistently demonstrates a higher GMPP compared to the other configurations. Under uniform shading conditions in Patterns 2, 5, 7, 9, and 19, all configurations yield the same GMPP. Conversely, the SP configuration stands out with the highest output in Patterns 3, 6, 8, and 19. Across most patterns, the TCT configuration consistently achieves the highest GMPP, while the SP configuration consistently achieves the lowest. All configurations yield the same results in instances of balanced shading in a row or column. However, in row-wise shading, the SP configuration outperforms the others. Overall, the TCT configuration is the superior performer in partially shaded conditions, while the SP configuration shines in uniformly shaded scenarios.

REFERENCES

[1] Garcia M, Vera JA, Marroyo L, Lorenzo E, Perez M. So- lar-tracking PV plants in Navarra: A 10 MW assessment. Progress in Photovoltaics: Research and Applications. 2009 Apr; 17(5):337–46.

[2] A. C. d. W. a. W. G. v. S. Boudewijn B. Pannebakker, Photovoltaics in the shade: one bypass diode per solar, PROGRESS IN PHOTOVOLTAICS: RESEARCH AND APPLICATIONS Prog. Photovolt: Res. Appl., 2017.

[3] M. G. VILLALVA, J. R. GAZOLI, E. RUPPERT F. Comprehensive approach to modeling and simulation of photovoltaic arrays, IEEE Transactions on Power Electronics, 2009 vol. 25, no. 5, pp. 1198--1208, ISSN 0885-8993

[4] Garcia M, Vera JA, Marroyo L, Lorenzo E, Perez M. Solar-tracking PV plants in Navarra: A 10 MW assessment. Progress in Photovoltaics: Research and Applications. 2009 Apr; 17(5):337–46

[5] Anuja Ingle, D.I. Sangotra, R.B. Chadge, Pratik Thorat, Module configurations in photovoltaic system: A review, Materials today proceedings vol 4, pp 12625-12629

[6] W. Xiao, W. G. Dunford, and A. Capel, "A novel modeling method for photovoltaic cells," in Proc. IEEE 35th Annu. Power Electron. Spec. Conf. (PESC), 2004, vol. 3, pp. 1950–1956.

[7] H. S. Rauschenbach, Solar Cell Array Design Handbook. NewYork: Van Nostrand Reinhold, 1980.

[8] J. A. Gow and C. D. Manning, "Development of a photovoltaic array model for use in power-electronics simulation studies," IEE Proc. Elect. Power Appl., vol. 146, no. 2, pp. 193–200, 1999.

[9] J. A. Gow and C. D. Manning, "Development of a model for photovoltaic arrays suitable for use in simulation studies of solar energy conversion systems," in Proc. 6th Int. Conf. Power Electron. Variable Speed Drives,1996, pp. 69–74.

[10] N. Pongratananukul and T. Kasparis, "Tool for automated simulation of solar arrays using general-purpose simulators," in Proc. IEEE Workshop Comput. Power Electron., 2004, pp. 10–14.

[11] S. Chowdhury, G. A. Taylor, S. P. Chowdhury, A. K. Saha, and Y. H. Song, "Modelling, simulation and performance analysis of a PV array in an embedded environment," in Proc. 42nd Int. Univ. Power Eng. Conf. (UPEC), 2007, pp. 781–785.

[12] J. Hyvarinen and J. Karila, "New analysis method for crystalline silicon cells," in Proc. 3rd World Conf. Photovoltaic Energy Convers., 2003, vol. 2, pp. 1521–1524.
[13] K. Nishioka, N. Sakitani,Y. Uraoka, and T. Fuyuki, "Analysis of multicrystalline silicon solar cells by modified 3-diode equivalent circuit model taking leakage current through periphery into consideration," Solar Energy Mater. Solar Cells, vol. 91, no. 13, pp. 1222–1227, 2007.
[14] C. Carrero, J.Amador, and S. Arnaltes, "A single procedure for helping PV designers to select silicon PV module and evaluate the loss resistances," Renewable Energy, vol. 32, no. 15, pp. 2579–2589, Dec. 2007.
[15] Ali, A. 2001.Macroeconomic variables as common pervasive risk factors and the empirical content of the Arbitrage Pricing Theory. Journal of Empirical finance, 5(3): 221–240.
[16] E. Koutroulis, K. Kalaitzakis, and V. Tzitzilonis. (2008). Development of a FPGA-based system for real-time simulation of photovoltaic modules, Microelectron. J. [Online].
[17] G. E. Ahmad, H. M. S. Hussein, and H. H. El-Ghetany, "Theoretical analysis and experimental verification of PV modules," Renewable Energy, vol. 28, no. 8, pp. 1159–1168, 2003.
[18] G. Walker, "Evaluating MPPT converter topologies using a matlab PV model," J. Elect. Electron. Eng., Australia, vol. 21, no. 1, pp. 45–55, 2001.
[19] M. Veerachary, "PSIM circuit-oriented simulator model for the nonlinear photovoltaic sources," IEEE Trans. Aerosp. Electron. Syst., vol. 42, no. 2, pp. 735–740, Apr. 2006.
[20] A. N. Celik and N. Acikgoz, "Modelling and experimental verification of the operating current of mono-crystalline photovoltaic modules using four- and five-parameter models," Appl. Energy, vol. 84, no. 1, pp. 1–15, Jan. 2007.
[21] Y.-C. Kuo, T.-J. Liang, and J.-F. Chen, "Novel maximum-power-pointtracking controller for photovoltaic energy conversion system," IEEE Trans. Ind. Electron., vol. 48, no. 3, pp. 594–601, Jun. 2001.
[22] M. T. Elhagry, A. A. T. Elkousy, M. B. Saleh, T. F. Elshatter, and E. M. Abou-Elzahab, "Fuzzy modeling of photovoltaic panel equivalent circuit," in Proc. 40th Midwest Symp. Circuits Syst., Aug. 1997, vol. 1, pp. 60–63.
[23] S. Liu and R. A. Dougal, "Dynamic multiphysics model for solar array," IEEE Trans. Energy Convers., vol. 17, no. 2, pp. 285–294, Jun. 2002.
[24] Y. Yusof, S. H. Sayuti, M. Abdul Latif, and M. Z. C. Wanik, "Modeling and simulation of maximum power point tracker for photovoltaic system," in Proc. Nat. Power Energy Conf. (PEC), 2004, pp. 88–93.
[25] D. Sera, R. Teodorescu, and P. Rodriguez, "PV panel model based on datasheet values," in Proc. IEEE Int. Symp. Ind. Electron. (ISIE), 2007, pp. 2392–2396.
[26] M. A. Vitorino, L. V. Hartmann, A. M. N. Lima, and M. B. R. Correa, "Using the model of the solar cell for determining the maximum power point of photovoltaic systems," in Proc. Eur. Conf. Power Electron. Appl., 2007, pp. 1–10.
[27] D. Dondi, D. Brunelli, L. Benini, P. Pavan, A. Bertacchini, and L. Larcher, "Photovoltaic cell modeling for solar energy powered sensor networks," in Proc. 2nd Int. Workshop Adv. Sens. Interface (IWASI), 2007, pp. 1–6.
[28] H. Patel and V. Agarwal, "MATLAB-based modeling to study the effects of partial shading on PV array characteristics," IEEE Trans. Energy Convers., vol. 23, no. 1, pp. 302–310, Mar. 2008.
[29] W.Yi-Bo,W. Chun-Sheng, L. Hua, andX.Hong-Hua, "Steady-state model and power flow analysis of grid-connected photovoltaic power system," in Proc. IEEE Int. Conf. Ind. Technol. (ICIT'08), pp. 1–6.
[30] K. Khouzam, C. Khoon Ly, C. Koh, and P. Y. Ng, "Simulation and realtime modelling of space photovoltaic systems," in Proc. IEEE 1st World Conf. Photovoltaic Energy Convers., Conf. Record 24th IEEE Photovoltaic Spec. Conf., 1994, vol. 2, pp. 2038–2041.
[31] M. C. Glass, "Improved solar array power point model with SPICE realization," in Proc. 31st Intersoc. Energy Convers. Eng. Conf. (IECEC), Aug. 1996, vol. 1, pp. 286–291.
[32] I. H. Altas and A. M. Sharaf, "A photovoltaic array simulation model for matlab–simulink GUI environment," in Proc. Int. Conf. Clean Elect. Power (ICCEP), 2007, pp. 341–345.
[33] E. Matagne, R. Chenni, and R. El Bachtiri, "A photovoltaic cell model based on nominal data only," in Proc. Int. Conf. Power Eng., Energy Elect. Drives, POWERENG, 2007, pp. 562–565.
[34] Y. T. Tan, D. S. Kirschen, and N. Jenkins, "A model of PV generation suitable for stability analysis," IEEE Trans. Energy Convers., vol. 19, no. 4, pp. 748–755, Dec. 2004.
[35] A. Kajihara and A. T. Harakawa, "Model of photovoltaic cell circuits under partial shading," in Proc. IEEE Int. Conf. Ind. Technol. (ICIT),2005, pp. 866–870. 1208 IEEE TRANSACTIONS ON POWER ELECTRONICS, VOL. 24, NO. 5, MAY 2009

[36] N. D. Benavides and P. L. Chapman, “Modeling the effect of voltage ripple on the power output of photovoltaic modules,” IEEE Trans. Ind.Electron., vol. 55, no. 7, pp. 2638–2643, Jul. 2008.

[37] W. De Soto, S. A. Klein, andW. A. Beckman, “Improvement and validation of a model for photovoltaic array performance,” Solar Energy, vol. 80, no. 1, pp. 78–88, Jan. 2006. Q. Kou, S. A. Klein, and W. A. Beckman, “A method for estimating the long-term performance of direct-coupled PV pumping systems,” Solar Energy, vol. 64, no. 1–3, pp. 33–40, Sep. 1998.

[38] A. Driesse, S. Harrison, and P. Jain, “Evaluating the effectiveness of maximum power point tracking methods in photovoltaic power systems using array performance models,” in Proc. IEEE Power Electron. Spec. Conf. (PESC), 2007, pp. 145–151.

[39] R. A. Messenger and J.Ventre, Photovoltaic Systems Engineering. Boca Raton, FL: CRC Press, 2004.

[40] F. Nakanishi, T. Ikegami, K. Ebihara, S. Kuriyama, and Y. Shiota, “Modeling and operation of a 10 kW photovoltaic power generator using equivalent electric circuit method,” in Proc. Conf. Record 28th IEEE Photovoltai Spec. Conf., Sep. 2000, pp. 1703–1706.

[41] J. Crispim, M. Carreira, and R. Castro, “Validation of photovoltaic electrical models against manufacturers data and experimental results,” in Proc. Int. Conf. Power Eng., Energy Elect. Drives, POWERENG, 2007, pp. 556–561. Woyte A, Nijs J, Belmans R. Partial shadowing of photovoltaic arrays with different system configurations: literature review and field test results. Solar Energy 2003; 74: 217–233.

[42] Fertig F, Rein S, Schubert M, Warta W. Impact of junction breakdown in muti-crystalline silicon solar cells on hot spot formation and module performance, Proceedings of the 26th European PV Solar Energy Conference and Exhibition, Hamburg, 2011; 1168–1178.

[43] Kurtz S. Photovoltaic module reliability workshop 2013, NREL/TP-5200-60167, NREL, Golden, 2013, http://www.nrel.gov/docs/fy14osti/60167.pdf (last accessed 5 March 2017).

[44] Köntges M, Kurtz S, Packard C, Jahn U, Berger KA, Kato K, Friesen T, Liu H, Van Iseghem M. Review of failures of photovoltaic modules, IEA-PVPS T13– 01:2014, International Energy Agency, 2014, http://iea-pvps.org/index.php?id=275 (last accessed 5 March 2017).